Pergamon

J. Aerosol Sci., Vol. 25, No. 4, pp. 699–709, 1994

0021-8502/94 $7.00 + 0.00

0021-8502(94)E0016-0

DEPOSITION OF PARTICLES IN TURBULENT PIPE FLOWS

K. W. LEE and J. A. GIESEKE

Battelle, 505 King Avenue, Columbus, OH 43201, U.S.A.

(*Received* 24 *September* 1992; *and in final form* 19 *January* 1993)

Abstract—Deposition rates of aerosol particles onto pipe walls under turbulent flow conditions were measured. Dioctyl phthalate (DOP) aerosols of six different sizes ranging from 0.035 to 1.3 μm were used in air flows whose Reynolds numbers were controlled at selected values between 1800 and 15,600. The turbulent inertial impaction, transition, and turbulent diffusion regimes were covered. The measured results show that the theory by Wells and Chamberlain (1967, *Brit. J. appl. Phys.* **18**, 1793) predicts deposition by diffusion in turbulent flows reasonably well, while the theory of Friedlander and Johnstone (1957, *Ind. Engr. Chem.* **49**, 1151) is suitable for correlating the data for deposition by inertial impaction. However, these theories alone were not satisfactory for estimating deposition rates in the neighborhood of the minimum aerosol deposition regime where both Brownian diffusional and inertial deposition mechanisms operate simultaneously.

INTRODUCTION

In general, deposition of aerosol particles from a flowing gas to an adjacent surface can result from particle inertia, gravitational settling, Brownian diffusion, thermophoresis, and electrical charge precipitation. For electrically neutral aerosols larger than about 1 μm in diameter, deposition from turbulent flow is due predominantly to particle inertia as was first shown by Friedlander and Johnstone (1957). As particle size becomes smaller than 1 micron, Brownian diffusion can also be important. The important deposition mechanisms from laminar flow for submicron aerosols are, however, Brownian diffusion and gravitational settling. Although there exist many experimental data available for turbulent flows, most of those cover either the turbulent inertia regime alone (Liu and Agarwal, 1974; Sehmel, 1968; Farmer *et al.*, 1970; Ilori, 1971; Alexander and Coldren, 1951; Postma and Schwendiman, 1960) or the turbulent diffusion regime (Gowariker, 1962). Very few studies were conducted covering both regimes. Therefore, very few experimental data points are available for the transient regime between the inertial and diffusional regimes, and the exact mechanisms controlling the regime are not fully known.

This paper reports a new set of experimental data on aerosol deposition from turbulent flows. Both the inertial and diffusional deposition regimes were covered. In order to help understand or study the deposition mechanisms, many experimental conditions including the particle size, the deposition tube size, and the Reynolds number were varied.

EXPERIMENTAL SYSTEM

Figure 1 is a schematic diagram of the system for measuring the aerosol deposition rates. The system consists of an aerosol generator, a deposition pipe and an aerosol detector. The different parts of the system are described below.

An aerosol generator that produces aerosols of moderately uniform sizes was used. The generator operates on the principle of vaporization and condensation of liquid material and comprises an atomizer, a vaporizer–condenser and a ^{85}Kr neutralizer. In this generator, a low vapor pressure substance such as DOP is dissolved in a volatile solvent, such as alcohol, and then the solution is dispersed using an atomizer. The polydisperse aerosol thus produced is then heated above the boiling point to evaporate. The vapor is subsequently allowed to cool and condense to form a monodisperse aerosol. The aerosol size is controlled by varying the concentration of DOP in the solution. This type of generator was previously

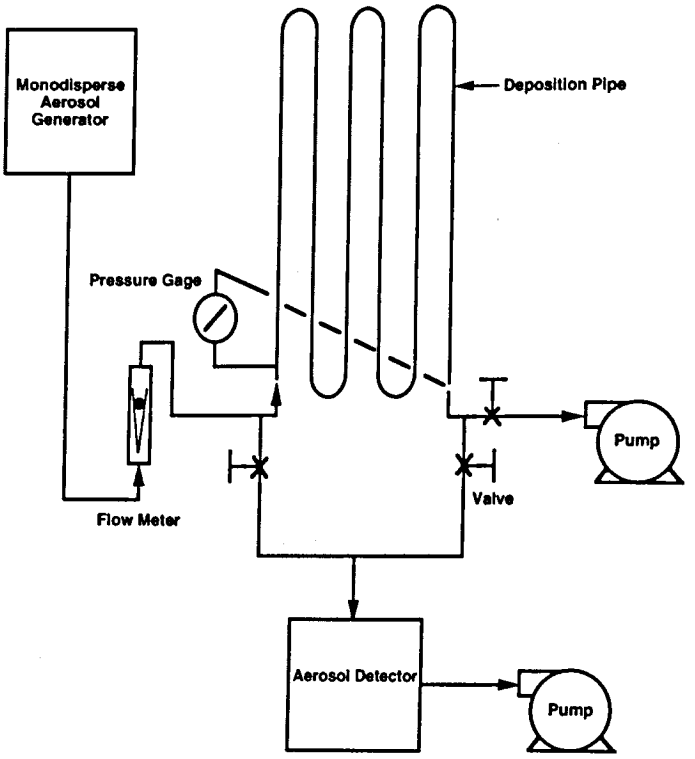

Fig. 1. Schematic diagram of the aerosol deposition measurement system.

reported by Liu and Lee (1975), and each component of the generator is briefly described here.

The atomizer used for the present study is capable of providing a constant aerosol output by means of a syringe pump. Compressed air at 35 psi was supplied to the atomizer through the inlet and was allowed to expand through an orifice consisting of a No. 80 (0.0135 in.) drill-sized hole. The DOP solution to be atomized was supplied to the jet through a 1.59 mm (1/16 in.) diameter tube. The coarse droplets produced by atomization impacted on the wall opposite the orifice and were drained off to a closed reservoir, while the fine spray left the atomizer at the top. With this arrangement, a stable aerosol was produced. However, the aerosol was polydisperse and the vaporizer–condenser described below was used to make the aerosol monodisperse.

The vaporizer and condenser section was made of a vertical glass tube of 19 mm diameter. The upper part of the tube was heated electrically by a heating tape with a power rating of 195 W at 115 V, but which was operated at 70 V. It was ensured that the temperature was maintained above the boiling point of DOP, which is 225°C. In passing through this heated section, the polydisperse DOP droplets vaporize. The vapor subsequently condenses to form uniform droplets in the lower section of the tube, which is cooled by free convection.

Since aerosols produced by atomization are expected to be electrically charged, they must be neutralized in order to avoid unwanted electrostatic effects. This was accomplished in the present case by exposing the aerosols to a cloud of bipolar ions produced by a radioactive source. The radioactive source, a 2 mCi ^{85}Kr source was placed inside an aluminum tube, and the aerosol was passed through the tube. The particles were thus brought to a state of Boltzmann charge equilibrium (Liu and Pui, 1974).

Two different copper tubes having fairly smooth inner surfaces were used as deposition pipes in the experiments. Pipes A and B used in the system had inside diameters (I.D.s) of 0.302 and 0.245 in. and lengths of 38.3 and 32.6 ft, respectively. It should be noted that the pipe lengths are designed to be relatively long since appreciable differences in the particle

concentrations upstream and downstream of the deposition pipes were sought for reliable data. In order to avoid any interference effects of aerosol deposition due to settling, each pipe was vertically incorporated into the system. Due to the rather long length of the tube and in order to accommodate them into the experimental set-up, there were 10 gradual 90° bends present in the set-up, as schematically shown in Fig. 1. In order to minimize the aerosol deposition interference due to these bends, the ratio of the bend curvature radius to the tube radius was designed to be sufficiently high at 15.

To determine the aerosol concentrations upstream and downstream of the deposition pipe, an electrical aerosol detector was used. This instrument is a simplified version of the electrical aerosol analyzer (Model 3030, Thermo-Systems, Inc., St. Paul, Minnesota), but it does not have an aerosol collection rod. Therefore, it can measure the total aerosol concentration without resolving the size distribution. The two essential parts of the instrument are the diffusion charger and the electrometer current sensor. The aerosol is detected by first exposing the particles to unipolar ions in the diffusion charger and then measuring the charge on the particles with the electrometer current sensor.

In addition, the instrument is equipped with a mass flow transducer, which can be used to measure aerosol flow rates of up to 60 l min^{-1}. The measurement can be made at different operating pressures. Details of this instrument have been described previously (Liu and Lee, 1976; Liu and Pui, 1974).

One of the main advantages of the electrical aerosol detector is that it allows the particle concentration to be measured over wide ranges of flow rates and pressures. In aerosol deposition studies, only the relative aerosol concentrations upstream and downstream of the pipe need to be measured, and the absolute aerosol concentration does not need to be known. The electrical aerosol detector is particularly suited for this purpose because it is basically a relative concentration measuring device, and the measurement can be made easily, quickly and with good accuracy.

FLOW AND AEROSOL DEPOSITION MEASUREMENTS

As a first check of the constructed system, the flow characteristics through the deposition tube were determined. Air at flow rates ranging from 1 to 70 l min^{-1} was passed through the pipes and the corresponding pressure drop was measured. The range of Reynolds numbers corresponding to these flow rates is between 200 and 15,600, thus covering both the laminar and turbulent flow regimes. The results for both pipes compared with existing theories are

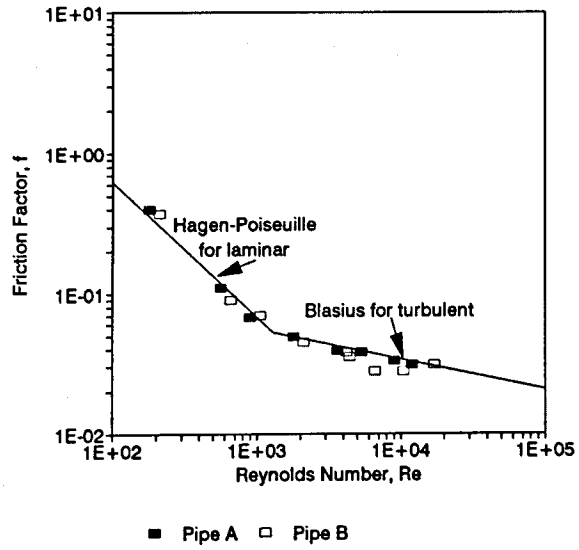

Fig. 2. Comparison of predicted and measured friction factors for pipes A and B (for predicted friction factors, see Schlichting 1968)

shown in Fig. 2. The theoretical predictions shown in the figures for the laminar and turbulent flow regimes, respectively (Schlichting, 1968), are as follows:

$$\Delta p = \frac{128 Q \mu L}{\pi d^4} \quad \text{(laminar flow)}, \tag{1}$$

where

Δp = pressure drop
μ = gas viscosity
L = pipe length
d = pipe diameter
Q = flow rate; and

$$\Delta p = f \frac{L}{d} \frac{\rho u^2}{2} \quad \text{(turbulent flow)}, \tag{2}$$

where

f = the friction factor ($=0.316/4\mathrm{Re}^{1/4}$)
ρ = gas density
u = gas velocity
Re = Reynolds number ($=ud\rho/\mu$).

The calculated pressure drop data for both pipes were converted into friction factors and compared with the experimental results. The comparison shows good agreement between the measured results and the corresponding prediction. It should be noted that the Blasius prediction of the pressure drop in turbulent flow is based on the smooth pipe surface. Therefore, the surface roughness of the tubes used in the current experiment can be considered essentially zero for the purpose of analyzing the aerosol deposition experimental data.

Aerosols of six different mean sizes were generated using a series of DOP solutions of different concentrations in alcohol. The number median diameters of these aerosols were 0.035, 0.05, 0.1, 0.3, 0.5 and 1.3 μm. The geometric standard deviation of the aerosols produced ranged from 1.2 to 1.8. Output of the aerosol generator was monitored over a 1 h period to verify suitable stability.

The procedure used for making aerosol deposition measurements consisted of controlling the flow at a desired rate, starting the aerosol generator and then measuring aerosol concentrations upstream and downstream of the deposition pipe using the electrical aerosol detector. One of the advantages of this experimental system was that the detector used in the experiment measures the relative concentration of aerosols with a real-time capability. Thus, the amount of aerosols deposited in the tube could be determined from the difference between the numbers of particles detected upstream and downstream of the pipe. The experimental results obtained using this technique (Method 1) were further verified by comparison with a technique in which aerosols are first tagged with a sodium fluorescein or uranine dye, and the aerosols deposited inside the tube as well as those passing through the tube were recovered manually by washing out the tube and by collecting the penetrated material on a filter. The amounts collected were then analyzed fluorometrically (Method 2).

Particle measurement results for both pipes A and B are shown in Table 1 and Figures 3 and 4. Also included with filled-in data points are the measurement results obtained using the washout method (Method 2). As a third method, both upstream and downstream aerosols were collected on membrane filters and analyzed with a fluorometer for selected cases (Method 3). These results are compared in Fig. 5 with the data obtained with the electrical aerosol detecting technique. It is noted that there is good agreement among the three methods. It can also be seen that particle deposition generally increases with increasing particle size and increasing flow velocity for larger particles, while no appreciable changes in deposition are observed for small particles.

One of the primary purposes of the present study was to determine deposition mechanisms appropriate for submicron particles passing through a pipe under turbulent flow

Table 1. Measurement results of particle deposition

Flow Rate (lpm)	Particle Dia. (μm)	Fraction Deposited	Reynolds No.	τ_+	v	v_+	Measurement Method
Pipe A, I.D.=0.767cm, L=1167 cm							
10	0.035	0.045	1808	1.90E-05	2.73E-03	9.72E-05	1
10	0.05	0.045	1808	3.89E-05	2.73E-03	9.72E-05	1
10	0.1	0.04	1808	1.55E-04	2.42E-03	8.62E-05	1
10	0.3	0.03	1808	1.40E-03	1.80E-03	6.43E-05	1
10	0.5	0.025	1808	3.89E-03	1.50E-03	5.34E-05	1
10	1.3	0.065	1808	2.63E-02	3.98E-03	1.42E-04	1
30	0.035	0.04	5424	1.30E-04	7.26E-03	9.88E-05	1
30	0.05	0.045	5424	2.66E-04	8.18E-03	1.11E-04	1
30	0.1	0.022	5424	1.06E-03	3.95E-03	5.39E-05	1
30	0.3	0.062	5424	9.57E-03	1.14E-02	1.55E-04	1
30	0.5	0.055	5424	2.66E-02	1.01E-02	1.37E-04	1
30	1.3	0.1	5424	1.80E-01	1.87E-02	2.55E-04	1
30	0.1	0.04	5424	1.06E-03	7.26E-03	9.88E-05	3
30	0.3	0.08	5424	9.57E-03	1.48E-02	2.02E-04	3
30	0.5	0.12	5424	2.66E-02	2.27E-02	3.10E-04	3
30	1.3	0.04	5424	1.80E-01	7.26E-03	9.88E-05	3
50	0.035	0.075	9041	3.18E-04	2.31E-02	2.01E-04	1
50	0.05	0.08	9041	6.50E-04	2.47E-02	2.15E-04	1
50	0.1	0.06	9041	2.60E-03	1.83E-02	1.60E-04	1
50	0.3	0.15	9041	2.34E-02	4.81E-02	4.19E-04	1
50	0.5	0.172	9041	6.50E-02	5.59E-02	4.87E-04	1
50	1.3	0.23	9041	4.39E-01	7.74E-02	6.75E-04	1
50	0.5	0.18	9041	6.50E-02	5.88E-02	5.12E-04	2
50	1.3	0.25	9041	4.39E-01	8.52E-02	7.43E-04	2
50	0.1	0.055	9041	2.60E-03	1.68E-02	1.46E-04	3
50	0.3	0.05	9041	2.34E-02	1.52E-02	1.32E-04	3
50	0.5	0.15	9041	6.50E-02	4.81E-02	4.19E-04	3
50	1.3	0.21	9041	4.39E-01	6.98E-02	6.08E-04	3
70	0.035	0.15	12657	5.74E-04	6.74E-02	4.37E-04	1
70	0.05	0.18	12657	1.17E-03	8.23E-02	5.34E-04	1
70	0.1	0.15	12657	4.68E-03	6.74E-02	4.37E-04	1
70	0.3	0.25	12657	4.22E-02	1.19E-01	7.74E-04	1
70	0.5	0.45	12657	1.17E-01	2.48E-01	1.61E-03	1
70	1.3	0.52	12657	7.92E-01	3.04E-01	1.98E-03	1
70	0.5	0.53	12657	1.17E-01	3.13E-01	2.03E-03	2
70	1.3	0.78	12657	7.92E-01	6.28E-01	4.08E-03	2
Pipe B, I.D.=0.622cm, L=993cm							
10	0.035	0.025	2229	4.17E-05	2.17E-03	5.23E-05	1
10	0.05	0.025	2229	8.52E-05	2.17E-03	5.23E-05	1
10	0.1	0.02	2229	3.41E-04	1.73E-03	4.17E-05	1
10	0.3	0.05	2229	3.07E-03	4.40E-03	1.06E-04	1
10	0.5	0.01	2229	8.52E-03	8.62E-04	2.08E-05	1
10	1.3	0.03	2229	5.76E-02	2.61E-03	6.29E-05	1
30	0.035	0.049	6686	2.85E-04	1.29E-02	1.19E-04	1
30	0.05	0.05	6686	5.82E-04	1.32E-02	1.22E-04	1
30	0.1	0.04	6686	2.33E-03	1.05E-02	9.67E-05	1
30	0.3	0.02	6686	2.10E-02	5.20E-03	4.79E-05	1
30	0.5	0.02	6686	5.82E-02	5.20E-03	4.79E-05	1
30	1.3	0.08	6686	3.94E-01	2.15E-02	1.98E-04	1
50	0.035	0.11	11144	6.98E-04	5.00E-02	2.94E-04	1
50	0.05	0.11	11144	1.42E-03	5.00E-02	2.94E-04	1
50	0.1	0.13	11144	5.70E-03	5.97E-02	3.52E-04	1
50	0.3	0.12	11144	5.13E-02	5.48E-02	3.23E-04	1
50	0.5	0.11	11144	1.42E-01	5.00E-02	2.94E-04	1
50	1.3	0.18	11144	9.63E-01	8.51E-02	5.01E-04	1
50	0.5	0.12	11144	1.42E-01	5.48E-02	3.23E-04	2
50	1.3	0.23	11144	9.63E-01	1.12E-01	6.60E-04	2
70	0.035	0.3	15601	1.26E-03	2.14E-01	9.39E-04	1
70	0.05	0.31	15601	2.57E-03	2.23E-01	9.77E-04	1
70	0.1	0.32	15601	1.03E-02	2.32E-01	1.02E-03	1
70	0.3	0.34	15601	9.24E-02	2.50E-01	1.09E-03	1
70	0.5	0.52	15601	2.57E-01	4.41E-01	1.93E-03	1
70	1.3	0.73	15601	1.73E+00	7.86E-01	3.45E-03	1
70	0.5	0.56	15601	2.57E-01	4.93E-01	2.16E-03	2
70	1.3	0.78	15601	1.73E+00	9.09E-01	3.99E-03	2

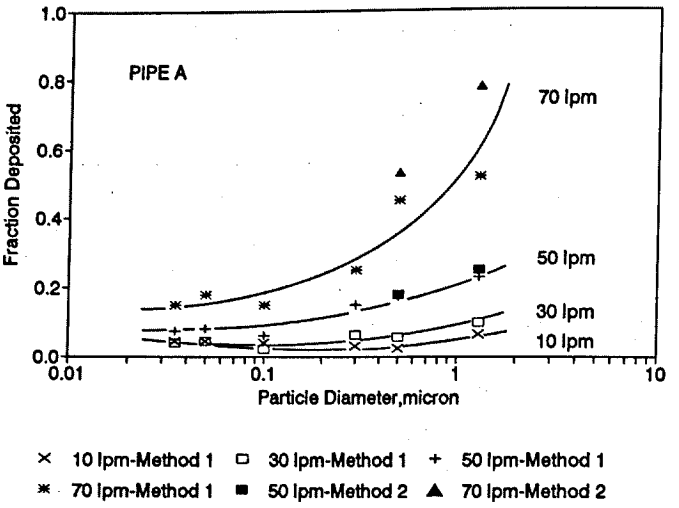

Fig. 3. Fraction of particles deposited as a function of particle size and flows for Pipe A (filled data were obtained from wash of tube and downstream filter sample).

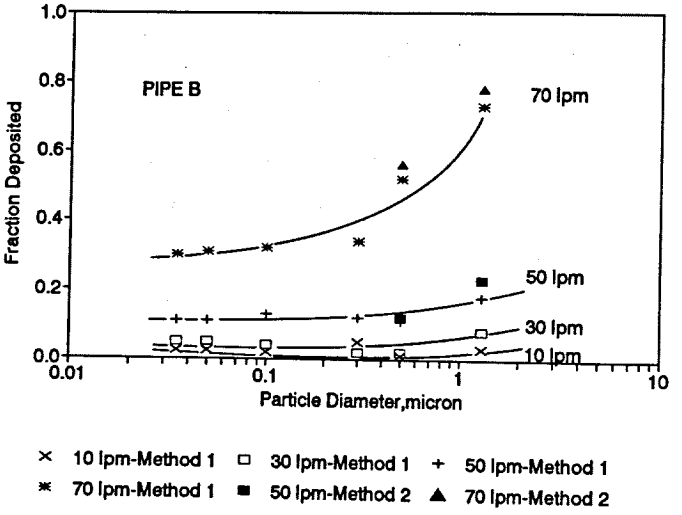

Fig. 4. Fraction of particles deposited as a function of particle size and flows for Pipe B (filled data were obtained from wash of tube and downstream filter sample).

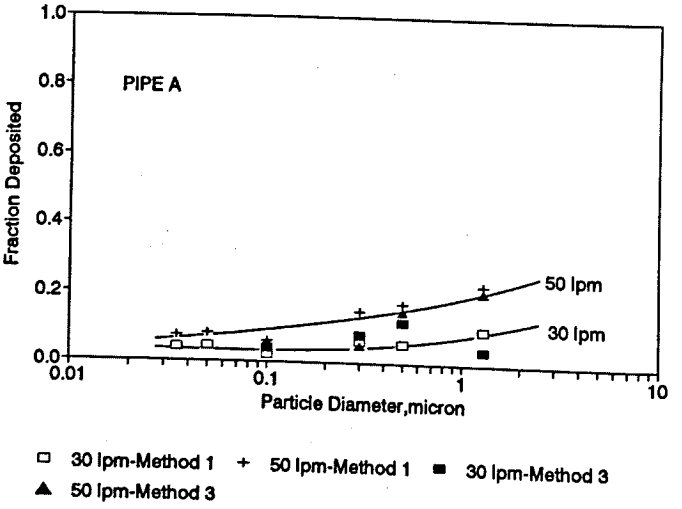

Fig. 5. Comparison of experimental data obtained by aerosol detector technique and by upstream and downstream filter measurements.

conditions. In order to identify appropriate mechanisms for variously sized aerosols at different flow velocities, the measured data were compared with existing theories.

COMPARISON WITH THEORIES

Particles passing through turbulent pipe flow may be deposited on surfaces by various mechanisms such as gravitation, electrostatic attraction, Brownian diffusion or inertial impaction. If particles are not excessively large and are electrically neutral, Brownian diffusion and inertial impaction are the only important deposition mechanisms.

In general, Brownian motion becomes important with decreasing particle size while deposition by inertial impaction increases as particle size increases. Therefore, there exists an intermediate range of particle sizes in which both deposition mechanisms of Brownian diffusion and inertial impaction operate, yet neither dominates.

Prediction of particle deposition due to Brownian diffusion under turbulent flow conditions was made previously by Davies (1966) and Wells and Chamberlain (1967). Turbulent flow may be divided into the three different flow regimes of turbulent core, buffer layer, and laminar sublayer. By calculating the transfer rate of particles diffusing by Brownian motion and by eddy diffusion through the above flow regimes, Davies obtained

$$V_{+d}=\frac{(\mathrm{Sc})^{-2/3}}{14.5\left(\frac{1}{6}\ln\frac{(1+\phi)^2}{1-\phi+\phi^2}+\frac{1}{\sqrt{3}}\arctan\frac{2\phi-1}{\sqrt{3}}+\frac{\pi}{6\sqrt{3}}\right)}, \tag{3}$$

where

$V_{+d}=(V/u_*)$=dimensionless particle deposition velocity due to diffusion
V=deposition velocity
$\mathrm{Sc}=(\nu/D)$=Schmidt number
$u_*=(f/2)^{1/2}u$=friction velocity
D=diffusion coefficient
ν=kinematic viscosity
$\phi=1/(2.9\sqrt[3]{D/\nu})$.

Wells and Chamberlain (1967) gave the following simple expression:

$$V_{+d}=0.2\,\mathrm{Sc}^{-2/3}\mathrm{Re}^{-1/8}. \tag{4}$$

Deposition due to inertial impaction mechanism was treated by many investigators such as Friedlander and Johnstone (1957), Davies (1966), Owen (1960) and Sehmel (1970).

Friedlander and Johnstone calculated the following particle deposition rate assuming that particles are carried from the mainstream by eddies:

$$V_{+i}=\frac{1}{\left(\frac{1}{\sqrt{f/2}}+\left(\frac{1525}{0.81\tau_+^2}-50.6\right)\right)} \quad \text{for } \tau_+<5.6 \tag{5}$$

$$V_{+i}=\frac{1}{\left(\frac{1}{\sqrt{f/2}}-13.73+5\ln\left(\frac{5.04}{\frac{\tau_+}{5.56}-0.959}\right)\right)} \quad \text{for } 5.6\le\tau_+<33.3$$

$$V_{+i}=\sqrt{f/2} \quad \text{for } \tau_+\ge 33.3,$$

where

$V_{+i}=(V/u_*)$=dimensionless particle deposition velocity due to inertial impaction
$\tau_+=(\tau u_*^2/\nu)$=dimensionless particle relaxation time
$\tau=(d_p^2\rho_p/18\mu)$=particle relaxation time
d_p=particle diameter
ρ_p=particle density.

The eddy diffusion coefficient for the fluid rather than particle was used. Upon reaching a point whose location is within the particle stopping distance from the pipe wall, a particle is assumed to make a free flight to the wall. The particle stopping distance was calculated assuming that particle velocity was 0.9 times the flow friction velocity. Davies proposed that the initial free-flight velocity be equal to the local fluctuating velocity. Liu and Ilori (1974) subsequently proposed the effective particle diffusivity accounting for eddy diffusivity and the inertial diffusivity.

The Davies theory of turbulent diffusion was compared with the experimental data obtained for small particles. In order to avoid the interferences due to the effects of inertial impaction, only data whose dimensionless relaxation time is less than 0.01 were used. To exclude the laminar flow regime, the data for $Re<2300$ were not included. Thus, the Reynolds number ranged from 5400 to 15,500, and the particle diameter ranged from 0.035 to 0.1 μm. The comparison showed that the experimental data were not correlated satisfactorily, showing wide spread of the data. A similar comparison was made with the Wells and Chamberlain (1967) theory. Figure 6 shows the comparison with the correlation by Wells and Chamberlain. Also included in the comparison in Fig. 6 are the data measured by Wells and Chamberlain (1967) and those reported by Gowariker (1962). It is seen that the present data fall between the two sets of data previously reported. Overall agreement between the theory and correlated data is considered to be satisfactory.

Figure 7 compares the experimental data for particles deposited due to inertial impaction with the theory of Friedlander and Johnstone (1957). Since these theories are good only for large particles, the data for which the dimensionless particle relaxation time is larger than 0.5 were included in the comparison. The experimental data from Liu and Agarwal (1974) are included. It is shown that the present experimental data agree reasonably well with those given by Liu and Agarwal and with the theory of Friedlander and Johnstone. It is noted that the following equation was used to calculate the dimensionless deposition velocity, V_+ from the measured deposited fraction, F

$$V_+ = \frac{-Q\ln(1-F)}{u_* \pi d L}. \tag{6}$$

In addition to verifying models for diffusional deposition from turbulent flow, an important objective of the present study was to measure the particle deposition in the transient regime, which lies between the diffusional and inertial impaction regimes. There exist no firm theories or adequate experimental data that quantitatively deal with particle

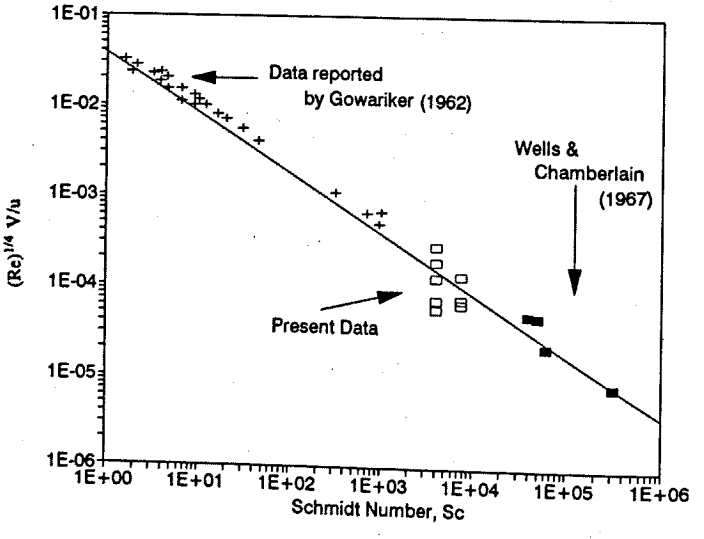

Fig. 6. Comparison of experimental data with correlation given by Wells and Chamberlain for diffusive deposition mechanism.

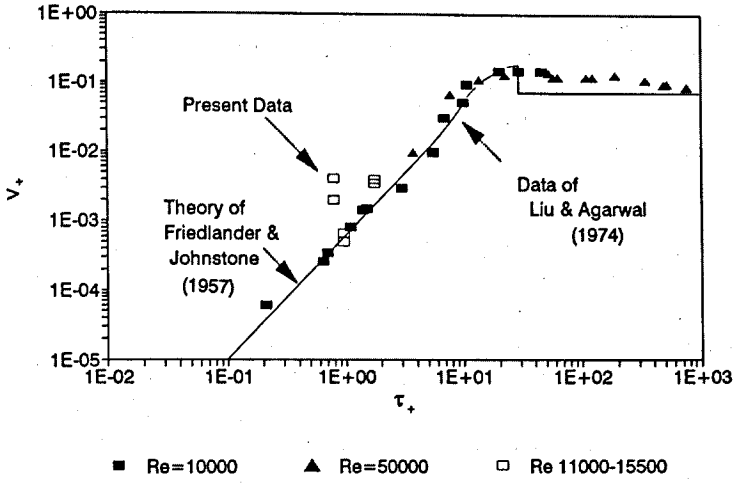

Fig. 7. Comparison of experimental data with theory for inertial impaction deposition mechanism.

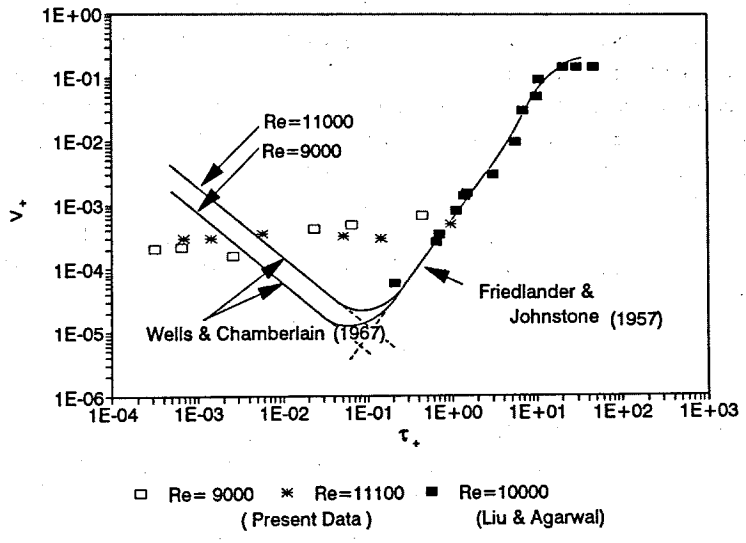

Fig. 8. Comparison of experimental data with theories for transient regime.

deposition in this regime. As discussed previously, except for the data used in the preceding comparison, most of the present data fall in the region in that both diffusional and inertial impaction mechanisms operate simultaneously, but neither dominates. One of the simple and common practices in predicting the particle deposition under this circumstance is to assume that both mechanisms are independent and additive. In order to investigate this possibility, the theories given by Wells and Chamberlain (1967) and by Friedlander and Johnstone (1957) have been added and are compared with the data in Fig. 8. The Reynolds number for the data shown in the figure ranges from 9000 to 11,000 and the corresponding dimensionless deposition velocity from the theory by Wells and Chamberlain (1967) is plotted for diffusional deposition. The theoretical prediction by Friedlander and Johnstone (1957) covering the inertial impaction shown in the figure is based on a Reynolds number of 10,000.

Although diffusional deposition velocity itself is a decreasing function of flow velocity, it is also seen to increase rather rapidly as the Reynolds number increases. This occurs, of course, because both V_+ and τ_+ include flow velocity through their nondimensionalization. It is noted that when the two theories are added, the measured deposition velocity is

underpredicted considerably. While the theories predict the existence of a rather sharp minimum deposition velocity, the experimental data are seen to be spread more broadly near the minimum. Similar comparisons for different flow conditions have been found to show the same trend. Therefore, it has been concluded that it is not sufficient to add diffusion and inertial impaction mechanisms to correlate the measured data in the transient regime.

In order to further observe the dependence of the deposition on flow velocity, the data were plotted as a function of Reynolds number alone. The results indicated that the deposition velocities increase sharply with increasing Reynolds numbers. However, it was noted that the particle size appeared to influence the deposition additionally. The experimental data were then plotted as a function of Stokes number alone. Stokes number is a dimensionless term describing the relative importance of particle inertial force to the fluid inertial force. No appreciable improvements in correlating the data were achieved. For a complete prediction of particle deposition velocities in the neighborhood between predominant mechanisms, or for quantitative interpretation of the discrepancy between prediction and measurement results, it may be necessary to investigate theoretically the mutual interference or synergistic effects of both mechanisms. Since the absolute values for dimensionless velocity are only on the order of 10^{-4} in this regime, it is also possible that the deposition mechanisms that are not considered important under normal conditions, i.e. deposition due to electrical charge attraction, might become comparable to the diffusion or inertial impaction mechanisms. Other possibilities are contributions to particle deposition from the effects of surface roughness of the pipes used or the effects of several bends present in the current experimental setup. However, further detailed analysis in terms of possible theories taking into account these additional mechanisms is beyond the scope of this study and remains a possibility for a future study. Therefore, an empirical correlation that accommodates the measured data within the experimental error has been sought. It was found that an additional term of $(2\times10^{-8}\,\mathrm{Re})$ added to the existing theories as shown below improves the correlation

$$V_{+t}=V_{+d}+V_{+i}+2\times10^{-8}\,\mathrm{Re}, \tag{7}$$

where V_{+t} is the combined dimensionless particle deposition velocity.

Figure 9 shows the experimental data whose dimensionless stopping distance ranges from about 0.001 to 1.0 and whose Reynolds number ranges from 5400 to 15,500 compared with the empirical correlation equation just discussed. The correlation equation is seen to underpredict somewhat the data whose Reynolds numbers are high.

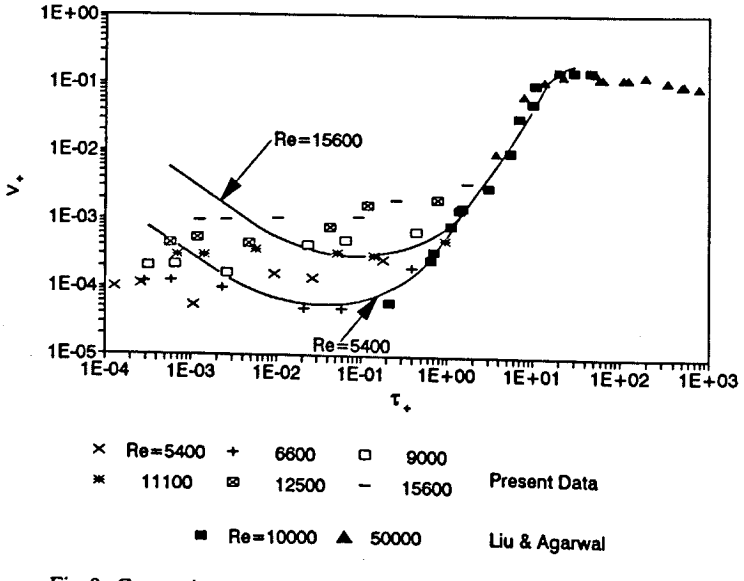

Fig. 9. Comparison of experimental data with correlation equation.

CONCLUSION

Particle deposition from turbulent flow to walls has been experimentally studied for particles in the submicron size range. The experimental results show that among the existing theories, the theory by Wells and Chamberlain (1967) and that by Friedlander and Johnstone (1957) are found to correlate satisfactorily the experimental data in the regimes of diffusional and inertial impaction deposition mechanisms, respectively. However, it is found that the usual practice of estimating deposition rates in the transition regime through use of the arithmetic sum of deposition velocities derived from these theories is not adequate. An additional empirical term has been identified that supplements the theories and gives improved agreement with the experimental data for predictive purposes.

Acknowledgements—Appreciation is due to Curtis Bridges who was instrumental in conducting the experiments and to C. Sue Jarrett and Mark A. Goldenberg who ran the computer programs for data analysis.

REFERENCES

Alexander, L. G. and Coldren, C. L. (1951) Droplet transfer from suspending air to duct walls. *Ind. Engr. Chem.* **43**, 1325.

Davies, C. N. (1966) *Aerosol Science*, pp. 393–446. Academic Press, London.

Farmer, R., Griffith, P. and Rohsenow, W. M. (1970) Liquid droplet deposition in two phase flow. ASME Paper No. 70-HT-1.

Friedlander, S. K. and Johnstone, H. F. (1957) Deposition of suspended particles from turbulent gas stream. *Ind. Engr. Chem.* **49**, 1151.

Gowariker, V. R. (1962) U.K. AEA, Report No. AERE M1055.

Ilori, T. A. (1971) Turbulent deposition of aerosol particles inside pipes. Ph.D. Thesis, University of Minnesota, Minneapolis, Minnesota.

Liu, B. Y. H. and Agarwal, J. K. (1974) Experimental observation of aerosol deposition in turbulent flow. *J. Aerosol. Sci.* **5**, 145.

Liu, B. Y. H. and Ilori, T. A. (1974) Aerosol deposition in turbulent pipe flow. *Envir. Sci. Technol.* **8**, 351.

Liu, B. Y. H. and Lee, K. W. (1975) An aerosol generator of high stability. *Am. Ind. Hyg. Assoc. J.* **36**, 861.

Liu, B. Y. H. and Lee, K. W. (1976) Efficiency of membrane and nuclepore filters for submicrometer aerosols. *Envir. Sci. Tech.* **10**, 345.

Liu, B. Y. H. and Pui, D. Y. H. (1974) Electrical neutralization of aerosols. *J. Aerosol Sci.* **4**, 465.

Liu, B. Y. H. and Pui, D. Y. H. (1975) On the performance of the electrical aerosol analyzer. *J. Aerosol Sci.* **6**, 249.

Owen, P. R. (1960) *Aerodynamic Capture of Particles*, pp. 8–75 Pergamon Press, Oxford.

Postma, A. K. and Schwendiman, L. C. (1960) Studies in micrometrics; particle deposition in conduits as a source of error in aerosol sampling. HW-65308, Hanford Laboratories.

Schlichting, H. (1968) *Boundary-Layer Theory*. McGraw-Hill, New York.

Sehmel, G. A. (1968) Aerosol deposition from turbulent airstreams in vertical conduits. BNWL-578, Pacific Northwest Laboratory.

Sehmel, G. A. (1970) Particle deposition from turbulent air flow. *J. geophys. Res.* **75**, 1766.

Wells, A. C. and Chamberlain, A. C. (1967) Transport of small particles to vertical surfaces. *Brit. J. appl. Phys.* **18**, 1793.